
Glucose Uptake, Perfusion, and Cell Proliferation in Head and Neck Tumors: Relation of Positron Emission Tomography to Flow Cytometry

U. Haberkorn, L. G. Strauss, Ch. Reisser, D. Haag, A. Dimitrakopoulou, S. Ziegler, F. Oberdorfer, V. Rudat, G. van Kaick

Institute of Radiology and Pathophysiology, German Cancer Research Center and Departments of Oto-Rhino-Laryngology, Department of Pathology, University of Heidelberg, Germany

The uptake of ^{18}F -Deoxyglucose (FDG) was studied in vivo in relation to the proliferation rate of human head and neck tumors. Forty-two patients with histologically proven squamous-cell carcinoma of the head and neck and four patients with metastases of head and neck tumors were examined with PET and FDG prior to surgery. In 35 of these patients, a flow cytometric analysis of the DNA content and the proliferation rate was done using one-dimensional flow cytometry (DAPI staining). In 17 cases, perfusion studies with ^{15}O -labeled water were performed. Twenty-seven specimens were evaluable by flow cytometry. The analysis of the distribution of the FDG uptake revealed two groups, showing a high and a lower uptake pattern. In both groups the FDG uptake and the proliferation rate were correlated with an r -value of 0.64 and 0.8 respectively. However, the slope of the regression function was flat. No correlation was found between the perfusion and the proliferation rate. It is suggested that these differences in uptake in histologically identical tumor populations may correspond to differences at the molecular level, e.g., differences in the amount of the glucose carrier, perhaps caused by oncogenic transformation.

J Nucl Med 1991; 32:1548-1555

The clinical staging of head and neck tumors depends mainly on the TNM classification. This is based on a clinical evaluation concerning the tumors size and extension and metastatic spread to lymph nodes or other organs. Biologic parameters of the tumor tissue are not included in the staging procedure. In a comparative study Feinmesser et al. found that computed tomography (CT) offers no advantage over physical examination (1). Morphologic parameters as size are not sufficient for an accurate estimation of the tumors aggressiveness. This may be provided by flow cytometry. Ploidy and proliferating activity are widely accepted as markers of the biological behavior of

malignant tumors (2,3). In a large series of cases with different tumor types, Atkin et al. observed that patients with a low (near-diploid) DNA index in general had a better survival rate (4). Ploidy and/or proliferation rate are reported to be correlated with clinical stage, survival or tendency for metastatic spread in head and neck tumors (5-8). On the other side, the FDG uptake could be correlated with histologic malignancy grading in brain tumors (9-12). Alavi et al. proposed that these data should be used to predict survival rates (13). Minn and coworkers report a strong correlation of the FDG uptake with the S-phase fraction and suggest that FDG imaging is a noninvasive method to assess the proliferative activity of human cancer (14). They used a conventional gamma camera in their study and therefore cross-sections were not available and the quantification was limited to ratios. Moreover, tumors with different histologies were included in this study. We evaluated the relation between the regional glucose uptake and the tumor proliferation rate in a large number of patients with squamous-cell carcinomas in order to determine the usefulness of positron emission tomography (PET) for the estimation of the tumors tendency to grow. Furthermore, tumor perfusion was assessed with ^{15}O -labeled water and compared to both FDG metabolism and flow cytometric data.

MATERIALS AND METHODS

PET

Forty-two patients with histologically proven squamous-cell carcinoma (scc) of the head and neck and four patients with lymph node metastases of head and neck scc were examined with PET prior to therapy. In 35 patients, specimens were obtained by biopsy from the examined region immediately after PET or during surgery 1 day after PET for further flow cytometric analysis. CT was performed in all cases prior to the PET study using a conventional CT scanner (Somatom DRH, Siemens, FRG). Continuous 8 mm thick sections were acquired (20-30 slices, parallel to the cantomeatal line) and skin markings were used for proper positioning in PET.

PET examinations were performed with a two ring detector system (PC2048-7WB Scanditronix, Sweden). Three PET sections (two primary and one cross-section) with a thickness of 11

Received Nov. 9, 1990; revision accepted Apr. 24, 1991.
For reprints contact: Uwe Haberkorn, MD, Institute of Radiology and Pathophysiology, German Cancer Research Center, Im Neuenheimer Feld 280, D-6900 Heidelberg, FRG.

mm were acquired. Each detector ring consists of 512 bismuth-germanate/gadolinium-orthosilicate detectors. The mean sensitivity of the system is 12500 cps/ μ Ci/cm³ for the primary and 17500 cps/ μ Ci/cm³ for the cross-section. FDG was used to assess the regional glucose uptake and phosphorylation. While the transport of FDG into the cell is comparable to glucose, FDG is trapped after the phosphorylation. Therefore, the distribution of FDG reflects the local glucose transport and phosphorylation in the tumor.

The patients were examined 1–2 hr after a light meal. One hour after intravenous administration of 350–444 MBq (9–12 mCi) FDG (12–15 mg total FDG), PET images were acquired for 10 min. In 8 patients a kinetic study was performed with 13 acquisitions for 1 hr. Transmission scans were performed prior to emission scanning with more than 10 million counts per section (⁶⁸Ge pin source; activity 185 MBq (5 mCi); dimensions: 60 mm length and 6 mm diameter; 16 rotations/min). The total number of counts in all cases exceeded 1 million.

The production of FDG was done according to a method described by Oberdorfer et al. (15). Thereafter the radiochemical purity was measured with high performance chromatography with values exceeding 98% (15).

Prior to the injection of FDG perfusion studies were performed in 18 of the 35 biopsied patients with ¹⁵O-labeled water (80–100 mCi). Five acquisitions each of 1 min duration were done.

PET images (average slice thickness: 11 mm) were generated by use of an iterative reconstruction program on a VAX 11/750 (Digital Equipment Corp Maynard, MA) (16). The image matrix was 128 × 128 and interpolated to 256 × 256 for display. The pixel size in all reconstructed images was 2 × 2 mm (spatial resolution 5.1 mm). The images were corrected for attenuation and scatter.

The identification of anatomic structures was done by comparing PET sections with the CT images. For quantitative evaluation, regions of interest (ROI) were defined in tumor and soft tissue with a region size exceeding 32 pixels in all cases. FDG uptake was then expressed as the standardized uptake value (SUV):

$$\text{SUV} = \frac{\text{tissue concentration (nCi/g)}}{(\text{injected dose (nCi)}/\text{body weight (g)})}$$

The SUV is a dimensionless parameter, which describes the relative distribution of a radiopharmaceutical. The ROIs were used for both, the ¹⁵O-water and FDG images. Tumor perfusion was evaluated from the image 5 min after bolus injection of ¹⁵O-water while the 10-min image 60 min after FDG application was used for the assessment of the glucose uptake. The uptake values for ¹⁵O-water were not analyzed using a compartment model, therefore these data may be semiquantitative. However, in a study with baboons Raichle et al. compared PET measurements of ¹⁵O-labeled water with a standard tracer technique based on intracarotid tracer injection (17). The values of both techniques were highly correlated. Moreover, the authors emphasized, that since the tissue concentration of the applied radionuclide is almost linearly related to the blood flow, the ¹⁵O image itself represents the distribution of the local tissue blood flow. Therefore, PET ¹⁵O-water images can be used to quantify tumor blood flow.

Blood samples were taken immediately before the injection of FDG and the blood glucose level was measured using a standard clinical laboratory kit.

Flow Cytometric Analysis

Small tissue samples obtained by biopsy or surgery were fixed immediately and stored in 96% ethanol until the DNA analysis. The preparation of suspensions of single-cell nuclei was done with scissors in a solution of 0.5% pepsin (1.5 Anson units per gram) in 0.9% saline after acidification with 0.25% hydrochloric acid. Thereafter the homogenate was supplemented with 2 ml pepsin solution and whirled 5 min at room temperature. After a sedimentation time of 2 min, 0.1–0.5 ml of the supernatant was injected into 8 ml of a fluorochrome solution, yielding about 10⁵ cell nuclei/ml. The DNA-specific fluorochrome solution consisted of 0.5 μ g DAPI (4'6-diamidino-a-phenylindole) and 20 μ g ribonuclease from bovine pancreas (100 Kunitz units/mg) per ml in 0.1-mol Tris buffer at pH = 7.6 (SERVA, Heidelberg, FRG).

The measurement of the nuclear DAPI fluorescence was performed after a staining time of 30 min using an IPC 22 pulse cytophotometer (PHYWE AG, Göttingen, FRG) with a UG1 and KV550 filter combination. For each probe, a total amount of at least 25,000 pulses was measured. The display and storage was done by use of a multichannel analyzer (MCA 8100, Canberra Industries, Meriden, CT). Further analysis was performed with a graphic computing system (Tektronix GS 4051 in combination with a 4662 digital plotter).

We performed the analysis of the DNA histograms in two steps according to Haag et al. (18): First the exponential correction for the superimposed background was subtracted from the counts in each channel. After subtraction the cleaned DNA distributions were drawn in the usual linear presentation.

For the analysis of the cell fractions in G_{0/1}, S and G₂ + M-phase, the curves of the cumulative frequencies of the corrected distributions were drawn by the plotter (G₀: quiescent cells; G₁: period between the last mitosis and the start of DNA replication; S: period of DNA synthesis G₂: period between the end of DNA replication and the start of the next mitosis; M: mitosis). Then the evaluation of the different cell fractions was performed graphically using a trapezoidal model (19) from the increments of the corresponding segments of the plotted curves. The proliferative index (PI) was calculated as:

$$\text{PI} = 100 \cdot (\text{S} + \text{G}_2 + \text{M}) / (\text{G}_{0/1} + \text{S} + \text{G}_2 + \text{M})$$

Furthermore, the specimens were classified by an experienced pathologist into three histologic grades: well-, moderately- and poorly-differentiated.

The results of the flow cytometric measurements and the PET data were evaluated using the t-test procedure and a cluster analysis (20). The same was done with the blood glucose level and the FDG uptake values.

RESULTS

The FDG uptake values in all 46 malignant lesions ranged from 1.8 to 6.0 SUV (normal neck muscles 0.8–1.0 SUV). The distribution of FDG uptake in primary tumors is shown in Figure 1. The perfusion values were in the range of 1.5 to 4.7 SUV (median 3.25 SUV, see Table 1).

Twenty-seven of 35 cases (23 tumors and 4 lymph node metastases) were evaluable in the flow cytometric study. Eight cases had to be excluded because of large necrotic

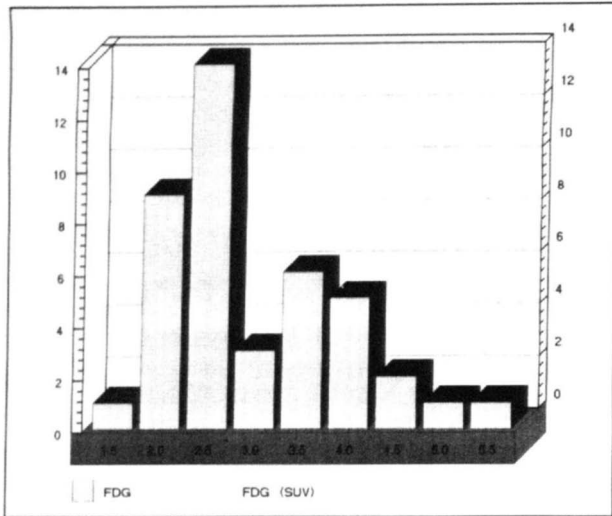


FIGURE 1. FDG uptake histogram in 42 patients with histologically proven squamous cell carcinoma of the head and neck. The x-axis represents the lower limits of the FDG uptake classes.

areas in the samples or due to sampling errors. Flow cytometry revealed PIs between 7.5 and 29.4% S + G₂/M cells (coefficient of variation between 2.6 and 6.2%; median 3.8%). In 17 of these 27 cases, PET data were available

TABLE 1
FDG and ¹⁵O Uptake (SUV), Proliferative Index (PI; in %), DNA Index (DI), and Tumor Localization in 27 Patients with Squamous-Cell Carcinoma of the Head and Neck

Patient no.	¹⁵ O	FDG	PI	DI	Localization
2523	1.53	2.63	22.3	2.3	o
163	2.11	2.47	22.1	1.5	o
2522	2.72	4.74	26.1	1.8	o
473	2.68	2.73	21.2	0.85	o
3008	2.94	4.05	13.9	1.8	h,l
235	3.08	2.42	16.9	2.05	o
469	3.36	2.28	12.4	1	l
150	4.41	4.41	19.3	1.5	o
739	3.68	2.51	13	1	o
533	3.8	3.84	7.5	1	l
615	4.51	2.96	23.1	1.65	o,h
977	3.85	2.84	24.8	1.5	h
983	2.96	2.5	23.1	1.65	o,h
1783	4.58	4.43	11.6	1.9	o,h
1032	4.72	2.89	32.2	1.6	h,l
1164	3.93	2.86	22.4	1.5	h,l
1373	2.73	3.95	17.7	1.4	l
1330		4.56	24.6	1.7	l
1404		3.84	12.6	1	l
1639		2.96	25.4	1.6	h,l
0054		2.81	29.5	1.7	h,l
621		2.4	7.8	1	o
1094		2.38	26.7	1.8	o,h
1331		4.59	29.9	1.7	m
1401		2.32	10.9	1.7	m
1440		2.29	20.6	1.9	m
1482		3.88	11.5	1	m

o = oropharynx, h = hypopharynx, l = larynx, m = metastasis.

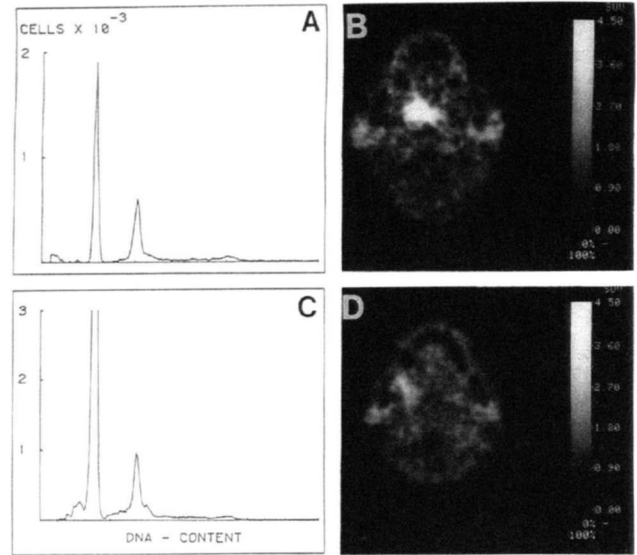


FIGURE 2. (A-B) PET images and (C-D) DNA histograms of two patients. Both showed comparable proliferation rates (2A: 26.1%; 2C: 26.7%), while the FDG uptake was significantly different (2B: 4.74 SUV; 2D: 2.38 SUV).

for the tumor perfusion. The data of PET and flow cytometry are summarized in Table 1.

The PET images and the DNA histograms of two patients are shown in Figure 2A-D. Although both tumors had comparable proliferation rates, the FDG uptake was significantly different. The time-activity curves for tumor and soft tissue in eight patients are shown in Figure 3. We noted an overlap of the curves only in the early uptake phase (= 10 min) of the radiopharmaceutical.

A significant correlation between H₂¹⁵O uptake and FDG uptake was not found. Furthermore, we observed no correlation between the H₂¹⁵O uptake and the PI (Fig. 4). Two groups were noted when the FDG uptake and PI were compared (Fig. 5). Both clusters showed a significant correlation between SUV and PI with $r = 0.64$ (regression function: $y = -110.77 + 83.8x - 12.7x^2$) in the lower uptake group and $r = 0.81$ ($y = 196 - 102.1x + 14x^2$) in the high uptake group (both significant at the 1% level). The distinct nature of the clusters was confirmed by cluster analysis using the weighted average linkage method with quadratic Euclidean distances. The DNA index and the FDG uptake showed a correlation of $r = 0.88$ (significant at the 1% level) in the group with the high uptake pattern and no correlation in the other group (Fig. 6). Furthermore, no correlation was found between the histologic grading (well-, moderately-, and poorly-differentiated) and the FDG uptake (Fig. 7). The FDG uptake was not dependent on the plasma glucose level; the results for 34 patients are shown in Figure 8.

DISCUSSION

In a study with rat brain tumors Watanabe et al. found a positive correlation between proliferation as measured

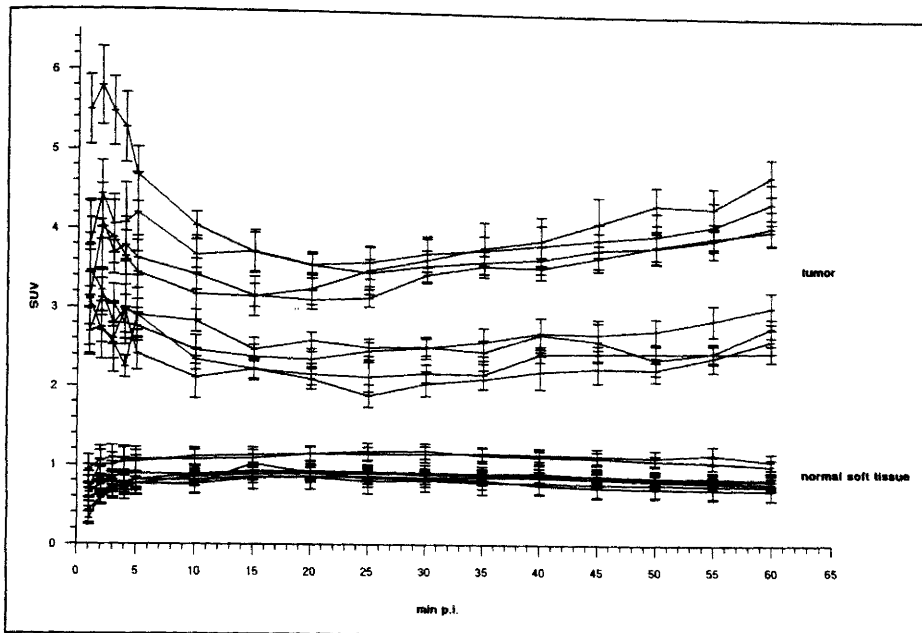


FIGURE 3. Time-activity curves (mean values and standard deviations) in eight patients for FDG uptake in tumors and normal soft tissue.

by the bromodeoxyuridine labeling index and the local cerebral glucose utilization (21). In their study, the distribution of cerebral blood flow did not correlate with the S-phase fraction. The findings in our patient study are comparable: no correlation between ^{15}O -labeled uptake and the proliferation rate was noted. Furthermore, the FDG uptake values showed no dependence on the perfusion as measured by PET.

From their animal experiments Watanabe et al. suggested that the increase in glucose utilization in these tumors is mainly needed for nucleic acid synthesis (21). Similar findings are reported by Minn et al., who found a high correlation between the FDG uptake and the S-phase fraction in patients (14). However, the tumor population in their study was inhomogeneous with respect to histology. Furthermore, the use of a gamma camera for data

acquisition and the tumor-to-contrast ratios did not permit an accurate quantification of activities in the tumors. Our own results in patients with scc of the head and neck demonstrate that there are two groups with a difference in FDG uptake but comparable proliferative activity. In general, this difference may be due to differences in the tumor histology or localization. All tumors were scc in the T3 or T4 stage. They were located in the oro- or hypopharynx without a particular location in one group as compared to the other. Another problem may be a difference in size, leading to a partial volume effect in the lower uptake group. However, this was not the case in our study, since the tumor size was not different for both groups. An unknown systematic error in the PET measurement is unlikely because of the large number of cases and the quality checks of the PET system. Moreover, the analysis of the FDG uptake data of all 42 patients with primary tumors gives evidence that there really are two groups with a different glucose uptake pattern.

Various methods are advocated for the estimation of the proliferative rate, including the labeling index using ^3H -thymidine (TLI), flow cytometric analysis of DNA or RNA content and the measurement of the Ki-67 antigen staining pattern. The TLI method requires the application of a radiolabeled compound and is only sensitive for S-phase cells. The biologic significance for the Ki-67 antigen is at present unsolved (22). Moreover van Dierendonck et al. found that nonproliferating cells may also retain the antigen pattern of the proliferation state for a longer period of time (23). Therefore, the Ki-67 staining is not in all cases a reliable measure of the proliferating cell fraction. The main problem of the flow cytometric analysis is the presence of background debris. This may result in differences between the flow cytometric values and the TLI

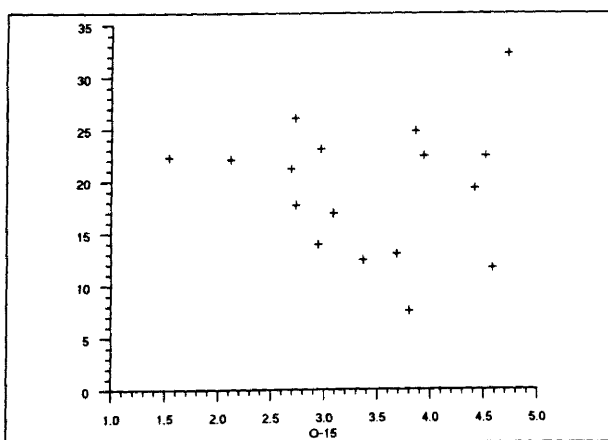


FIGURE 4. Uptake of ^{15}O -labeled water (SUV) in relation to the proliferative index (%) in 17 patients.

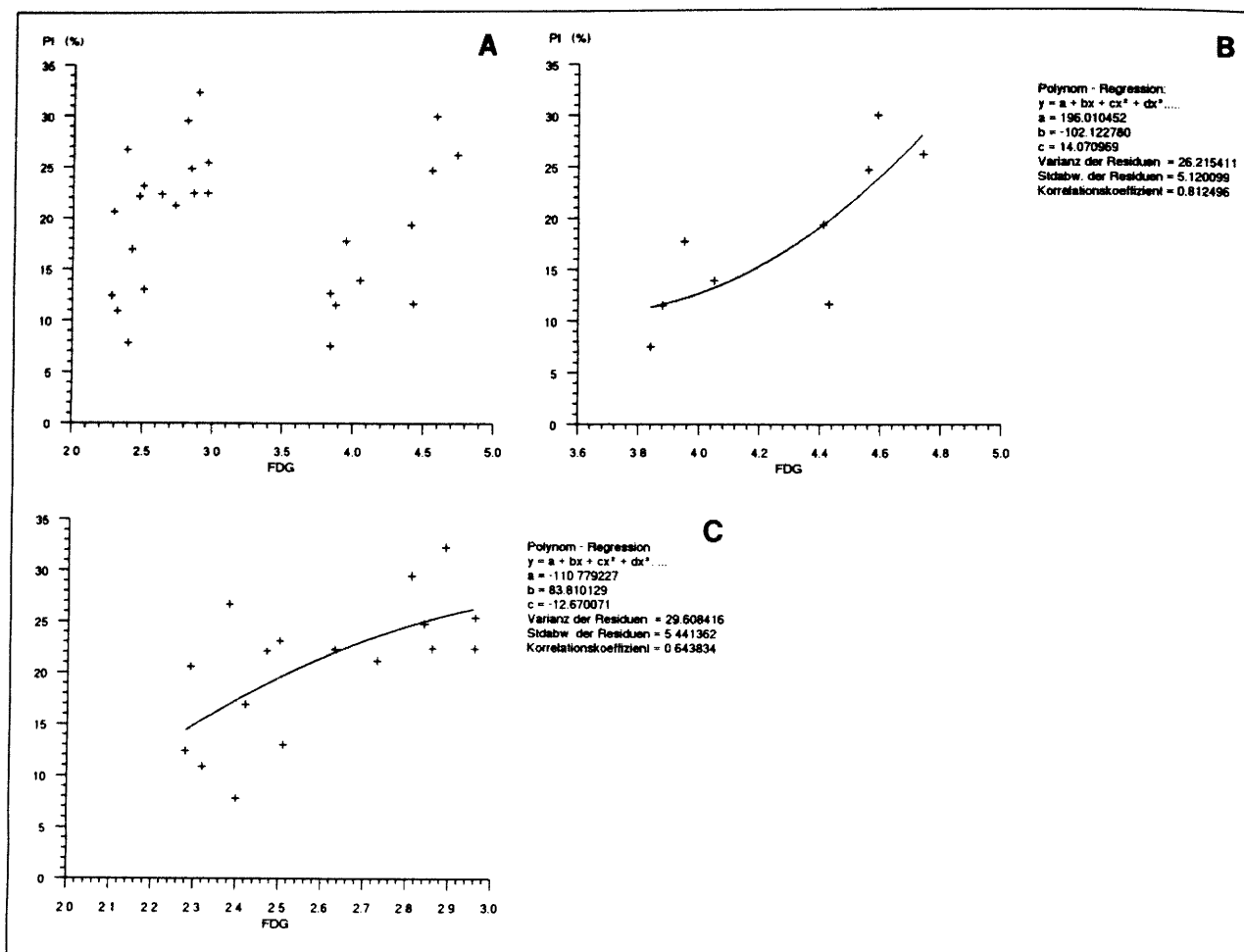


FIGURE 5. (A-C) Relation of the proliferative index (%) to FDG uptake (SUV). Two groups are identified, one with a higher (5B; $r = 0.81$; $p < 0.01$) and one with a lower (5C; $r = 0.64$; $p < 0.01$) uptake.

(17). However, as demonstrated by Haag et al., these differences are compensated by an appropriate subtraction of the background levels (18). Therefore flow cytometry is a reliable reference method.

The influence of the glucose content in the surrounding medium on the uptake into the cell is studied mainly in cultures of chicken fibroblasts. Amos and coworkers suggest, that glucose itself acts as a repressor of the glucose uptake (24). This is probably achieved either by blocking of the carrier synthesis at a post-transcriptional level or by inactivation of the carrier by a protein in combination with a cofactor product of the glucose metabolism (protein-A-cofactor-inactivator model). Tumor cells are thought to be independent of the glucose content of the medium. In experimental tumors, Yamada et al. found no influence of the plasma glucose level on the glucose uptake (25). Data from a study with recurrent colorectal cancer showed only a low correlation (26). In this series, we found no significant correlation between glucose-plasma level and the FDG uptake. Since the blood samples were taken immediately before the injection of FDG and the uptake

values 1 hr after injection were chosen for quantitative evaluation, we had to assume that there were no major changes in the plasma glucose level during the first 30 min.

One explanation for the two clusters deals with the karyotypic progression in tumors. It has been hypothesized, that in tumors a sequential emergence of mutant subpopulations with increasing malignant properties exists. Chromosome instabilities can predispose to further aberration within tumors (27). The group showing the high uptake pattern may represent a later stage of chromosome aberration. However, the PI and the DI in both groups revealed comparable values. Moreover, it is known that an increase in glucose uptake is one of the early features of malignant transformation (28-32). Increase in glucose uptake is an early event in carcinogenesis, not a change in later stages of tumor progression.

The results of Watanabe and Minn suggested that the glucose uptake is increased due to the needs for nucleic acid synthesis and therefore is directly related to the tumors tendency to grow (14,21). However, this is a very simple

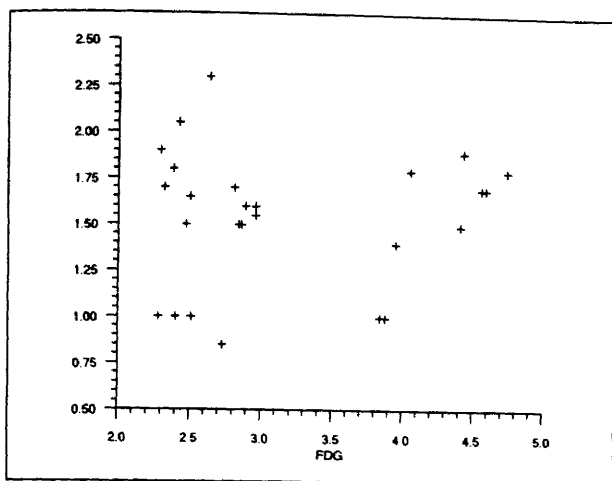


FIGURE 6. FDG uptake and DNA index. The high uptake group is highly correlated ($r = 0.88$), the low uptake group shows no correlation.

explanation. Nutrient supply may be the limiting factor of cell growth in arresting the cells in the early G_1 or G_0 phase of the cycle (33). This is only the situation in the case of insufficient nutrient supply for the completion of the cell cycle. Barsh et al. found, however, that the increase in membrane transport and the size of the intracellular glucose pool are dissociated from the increase of DNA synthesis and cell growth (34). Similar results were obtained by Weber et al. (35). They observed that the increase in glucose transport rate exceeds the requirements for growth when compared to the uptake of other growth-related substances, such as potassium and amino acids. Moreover, cells transformed by Rous sarcoma virus and proliferating at the same rate than normal control cells, transported hexoses at a four- to five-fold higher rate than the controls (35). Our data reveal a correlation in both uptake groups, but it is important to note, that the slope of the regression

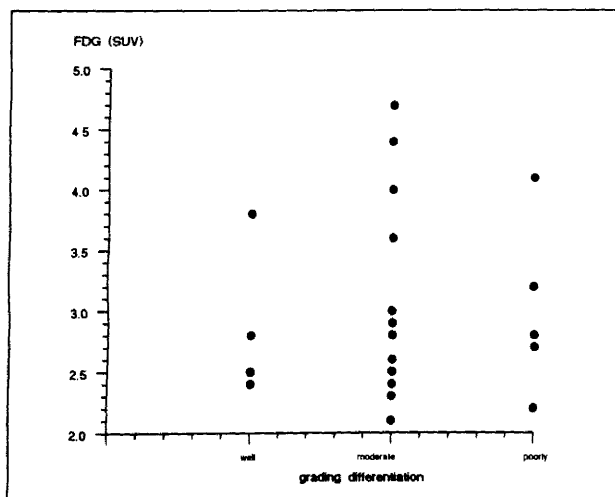


FIGURE 7. Comparison of the histologic grading and the FDG uptake in 20 patients. No correlation is observed.

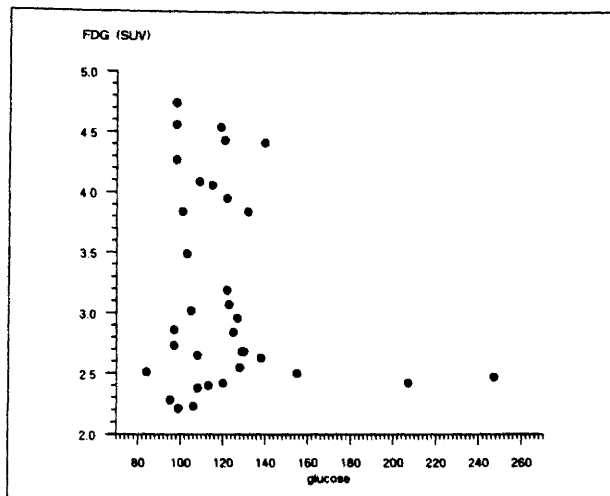


FIGURE 8. Glucose-plasma level and FDG uptake in 34 patients. No influence of the glucose-plasma level on the FDG uptake is seen.

function is flat. Large changes in the proliferation rate result in only moderate changes in FDG uptake. This suggests that indeed the glucose uptake is not directly regulated by the needs for DNA synthesis.

Most observers agree that in transformed cells there is mainly an increase in V_{max} of the transport (30,31,36). This is explained by an increased number of transporters in the cell membrane (31,37,38). Our kinetic data (Fig. 3) revealed a clear difference of the time activity curves beginning at 10 minutes after the injection of FDG, indicating that this difference is mainly caused by transport phenomena. Several causes exist for elevated glucose carriers. White et al. found that the elevation of these carriers in chicken cells transfected with src oncogene was due to a reduction in the rate of the degradation of the protein, whereas rat fibroblasts showed an increase in mRNA encoding the transport protein (39). Flier et al. demonstrated that elevated transport protein and mRNA levels are present in rat fibroblasts when transfected with src or ras oncogene (40). Differences in the amount of mRNA for the HepG2 transporter were also found in hepatoma cells and normal liver cells with an increased rate in the hepatoma cells (29). In a recent study, Yamamoto et al. found elevated amounts of the erythrocyte glucose transporter mRNA in a variety of human cancer tissues, including hepatoma, pancreatic cancer, esophageal cancer and colon cancer (41). Therefore, the underlying molecular mechanism for the different FDG uptake in the two groups of head and neck tumors may be due to a different transcription and translation of the glucose carrier gene.

The difference between the two uptake groups can be related to different amounts of the glucose transport protein, but this still remains to be explained. Perhaps this difference is due to a varying production of oncoproteins, causing changes in metabolic activity. The results of White,

Flier, and others with src or ras oncogene give evidence for this hypothesis (32,39,40,42). Weber observed an increased number of glucose carriers in the cell membrane in Rous sarcoma virus-transformed cells (38). The increase of the carrier was dependent on the activity of the pp60-src. Furthermore, it is known that an elevated expression of multiple oncogenes, including Ha-ras, Ki-ras, and myc is associated with highly aggressive tumors of the head and neck (43,44). Therefore, PET with FDG may reflect the regulation or dysregulation of the FDG metabolism at the molecular level.

In conclusion, our study suggests, that the glucose uptake in scc of the head and neck is correlated with the proliferative activity of a tumor. However, there are two groups, indicating that in addition to a dependence of glucose uptake on the growth rate other mechanisms also are involved. These results and the results of a variety of cell experiments give evidence for a difference in glucose carrier expression, perhaps due to oncogenic alterations.

REFERENCES

- Feinmesser R, Freeman JL, Noyek AM, Birt D. Metastatic neck disease—a clinical/radiographic/pathologic correlative study. *Arch Otolaryngol Head Neck Surg* 1987;113:1307–1310.
- Friedlander ML, Hedley DW, Taylor JW. Clinical and biological significance of aneuploidy in human tumors. *J Clin Pathol* 1984;37:961–974.
- Merkel DE, McGuire WL. Ploidy, proliferative activity and prognosis. DNA flow cytometry of solid tumors. *Cancer* 1990;65:1194–1205.
- Atkin NB, Kay R. Prognostic significance of modal DNA values and other factors in malignant tumors, based on 1465 cases. *Br J Cancer* 1979;40:210–221.
- Ensley JF, Maciorowski Z, Hassan M, et al. Cellular DNA content parameters in untreated and recurrent squamous-cell cancers of the head and neck. *Cytometry* 1989;10:334–338.
- Holm LE. Cellular DNA amounts of squamous cell carcinomas of the head and neck region in relation to prognosis. *Laryngoscope* 1982;92:1064–1069.
- Johnson TS, Williamson KD, Cramer MM, Peters LJ. Flow cytometric analysis of head and neck carcinoma DNA index and S-fraction from paraffin-embedded sections: comparison with malignancy grading. *Cytometry* 1985;6:461–470.
- Brauneis JW, Laskawi R, Schröder M, Göhde W. Ergebnisse der Impulszytometrie bei malignen Tumoren des Kopf-Hals-Bereiches. *HNO* 1987;37:369–372.
- DiChiro G, DeLaPaz R, Brooks R, et al. Glucose utilization of cerebral gliomas measured by (¹⁸F)fluorodeoxyglucose and positron emission tomography. *Neurology* 1982;32:1323–1329.
- DiChiro G, Hatazawa J, Katz DA, Rizzoli HV, DeMichele DJ. Glucose utilization by intracranial meningiomas as an index of tumor aggressivity and probability of recurrence: a PET study. *Radiology* 1987;164:521–526.
- Kornblith PL, Cummins CJ, Smith BH, Brooks RA, Patronas NJ, DiChiro G. Correlation of experimental and clinical studies of metabolism by PET scanning. *Prog Exp Tumor Res* 1984;27:170–178.
- Mineura K, Yasuda T, Kowada M, Shishido F, Ogawa T, Uemura K. Positron emission tomographic evaluation of histological malignancy in gliomas using oxygen-15 and fluorine-18-fluorodeoxyglucose. *Neurological Res* 1986;8:164–168.
- Alavi JB, Alavi A, Chawluk J, Kushner M, et al. Positron emission tomography in patients with glioma. A predictor of prognosis. *Cancer* 1988;62:1074–1078.
- Minn H, Joensuu H, Ahonen A, Klemi P. Fluorodeoxyglucose imaging: a method to assess the proliferative activity of human cancer in vivo. Comparison with DNA flow cytometry in head and neck tumors. *Cancer* 1988;61:1776–1781.
- Oberdorfer F, Hull WE, Traving BC, Maier-Borst W. Synthesis and purification of 2-deoxy-2-¹⁸F-fluoro-D-glucose and 2-deoxy-2-¹⁸F-fluoro-D-mannose: characterization of products by ¹H- and ¹⁹F-NMR spectroscopy. *Int J Appl Radiat Isot* 1986;37:695–701.
- Schmidlin P, Kübler WK, Doll J, Strauss LG, Ostertag H. Image processing in whole body positron emission tomography. In: Schmidt HAE, Csernay L, eds. *Nuklearmedizin*. Stuttgart: Schattauer; 1987:84–87.
- Raichle ME, Martin WRW, Herscovitch MP, Mintun MA, Markham J. Brain blood flow measured with intravenous H₂¹⁵O. II. Implementation and validation. *J Nucl Med* 1983;24:790–798.
- Haag D, Feichter G, Goertler K, Kaufmann M. Influence of systematic errors on the evaluation of the S phase portions from DNA distributions of solid tumors as shown for 328 breast carcinomas. *Cytometry* 1987;8:377–385.
- Ritch PS, Schackney SE, Schuette WH, Talbot TL, Smith CA. A practical graphical method for estimating the fraction of cells in S in DNA histograms from clinical tumor samples containing aneuploid cell populations. *Cytometry* 1983;4:66–74.
- Sachs L. *Angewandte Statistik*. Berlin: Springer; 1984:329–333.
- Watanabe A, Tanaka R, Takeda N, Washiyama K. DNA synthesis, blood flow, and glucose utilization in experimental rat brain tumors. *J Neurosurg* 1989;70:86–91.
- Sasaki K, Murakami T, Kawasaki M, Takahashi M. The cell cycle associated change of the Ki-67 reactive nuclear antigen expression. *J Cell Physiol* 1987;133:579–584.
- van Dierendonck JH, Keijzer R, van de Velde CJH, Cornelisse CJ. Nuclear distribution of the Ki-67 antigen during the cell cycle: comparison with growth fraction in human breast cancer cells. *Cancer Res* 1989;49:2999–3006.
- Amos H, Musliner TA, Asdourian H. Regulation of glucose carriers in chick fibroblasts. *J Supramolecular Structure* 1977;7:499–513.
- Yamada K, Matsuzawa T, Endo S, et al. Differences in glucose metabolism among brain, myocardium and tumor. In: Matsuzawa T, ed. *Proceedings of the International Symposium on current and future aspects of cancer diagnosis with positron emission tomography*. Sendai, Japan: Tohoku University, 1985:28–33.
- Haberhorn U, Strauss LG, Dimitrakopoulou A, et al. PET studies of FDG metabolism in patients with recurrent colorectal tumors receiving radiotherapy. *J Nucl Med* 1991;32:1485–1490.
- Wolman SR. Karyotypic progression in human tumors. *Cancer Metastasis Rev* 1983;2:257–293.
- Birnbaum MJ, Haspel HC, Rosen OM. Transformation of rat fibroblasts by FSV rapidly increases glucose transporter gene transcription. *Science* 1987;235:1495–1498.
- Flier JS, Mueckler M, McCall AC, Lodish HF. Distribution of glucose transporter messenger RNA transcripts in tissues of rat and man. *J Clin Invest* 1987;79:657–661.
- Hatanaka M. Transport of sugars in tumor cell membranes. *Biochim Biophys Acta* 1974;355:77–104.
- Inui KI, Tillotson LG, Isselbacher KJ. Hexose and amino acid transport by chicken embryo fibroblasts infected with temperature-sensitive mutant of rous sarcoma virus. *Biochim Biophys Acta* 1980;598:616–627.
- Godwin AK, Lieberman MW. Early and late responses to induction of ras T24 expression in Rat-1 cells. *Oncogene* 1990;5:1231–1241.
- Holley RW, Kiernan JA. Control of the initiation of DNA synthesis in 3T3 cells: low-molecular weight nutrients. *Proc Natl Acad Sci USA* 1974;71:2942–2945.
- Barsh GS, Cunningham DD. Nutrient uptake and control of animal cell proliferation. *J Supramolecular Structure* 1977;7:61–77.
- Weber MJ, Evans PK, Johnson MA, McNair TF, Nakamura KD, Salter DW. Transport of potassium, amino acids and glucose in cells transformed by Rous sarcoma virus. *Fed Proc Fed Am Soc Exp Biol* 1984;43:107–112.
- Weber MJ. Hexose transport in normal and in Rous sarcoma virus-transformed cells. *J Biol Chem* 1973;248:2978–2983.
- Salter DW, Baldwin SA, Lienhard GE, Weber MJ. Proteins antigenetically related to the human erythrocyte glucose transporter in normal and Rous sarcoma virus-transformed chicken embryo fibroblasts. *Proc Natl Acad Sci USA* 1982;79:1540–1544.
- Weber MJ, Nakamura KD, Salter DW. Molecular events leading to enhanced glucose transport in Rous sarcoma virus-transformed cells. *Federation Proc* 1984;43:2246–2250.
- White MK, Weber MJ. Transformation by the src oncogene alters glucose transport into rat and chicken cells by different mechanisms. *Mol Cell Biol* 1988;8:138–144.
- Flier JS, Mueckler MM, Usher P, Lodish HF. Elevated levels of glucose transport and transporter messenger RNA are induced by ras or src oncogenes. *Science* 1987;235:1492–1495.

41. Yamamoto T, Seino Y, Fukumoto H, et al. Over-expression of facilitative glucose transporter genes in human cancer. *Biochem Biophys Res Comm* 1990;170:223-230.
42. Sistonen L, Hölttä E, Mäkelä TP, Keski-Oja J, Alitalo K. The cellular

- response to induction of the p21c-Ha-ras oncoprotein includes stimulation of jun gene expression. *EMBO J* 1989;9:815-822.
43. Field JK, Lamothe A, Spandidos DA. Clinical relevance of oncogene expression in head and neck tumors. *Anticancer Res* 1986;6:595-600.

EDITORIAL

PET Cancer Evaluations with FDG

A high rate of glycolysis is a biochemical hallmark of many types of aggressive tumors, a phenomenon first described in the now widely cited work of Warburg et al. (1,2) and validated by others (3). Like many scientific discoveries, some of the practical implications of this observation were to remain undefined for a period of time. The development of the autoradiographic ^{14}C -deoxyglucose technique by Sokoloff and colleagues (4) followed by the extension of the method to human studies with 2-[^{18}F] fluoro-2-deoxy-D-glucose (FDG) and PET (5-7) made possible the first in vivo cross-sectional evaluations of glucose utilization in health and disease. One of the first clinical applications of PET FDG imaging was the evaluation of astrocytomas, a field pioneered by Di Chiro and colleagues at the NIH (8,9).

Di Chiro et al. (10,11) demonstrated that a high glycolytic rate of high-grade astrocytomas effectively differentiates them from low-grade astrocytomas. Diagnostically, preoperative PET FDG studies of brain tumor patients permit accurate histological grading of the lesions and often has implications for surgical and other therapeutic approaches. Postoperatively, PET FDG studies of brain tumor patients are utilized to monitor the progression of residual tumor and to differentiate radiation necrosis from recurrent tumors (12). Several investigators have also shown that the relative rate of glucose utilization of brain tumors mapped by PET FDG

images also has prognostic significance: length of survival is inversely correlated with FDG uptake in some series (13).

It is now widely recognized that PET FDG brain tumor imaging is useful diagnostically for grading lesions noninvasively and is also effective in monitoring disease progression and, potentially, response to therapy.

In addition to PET FDG imaging of brain tumors, other oncologic applications of the PET FDG method have emerged. Primary lesions studied with FDG have included head and neck tumors [evaluated with a specially collimated gamma camera (14) and PET (15)], lung carcinomas (16), lymphoma (17), breast carcinomas [PET FDG (18,19) and gamma camera FDG studies (20)], colorectal carcinomas (21,22), thyroid cancer [imaged with a gamma camera and FDG (23)], and musculoskeletal tumors (24).

The accelerated glycolytic rate of malignant tumors is associated with increased activities of rate-controlling enzymes for glycolysis, including hexokinase, phosphofructokinase and pyruvate dehydrogenase (1,2). Investigations have demonstrated a relationship between the magnitude of the increase in the glycolytic rate and the rate of tumor growth (3), and the neoplastic transformation of some cell lines is associated with increased membrane glucose transport capability (25). Initial studies by Minn et al. (14,20) revealed a relationship between glucose metabolism and the proliferative activity of breast, head and neck tumors based on DNA flow cytometry data. Minn also demonstrated decreased FDG uptake in 17 of 19 patients with malignant head

and neck tumors who responded to radiation therapy.

In the large majority of reported cases, both untreated primary and metastatic lesions have had high levels of glycolysis reflected by high levels of FDG uptake. These initial studies have established the potential of PET FDG imaging as a tumor localization procedure and have produced interesting insights into the prognostic and therapeutic implications of FDG uptake in tumors.

In this issue of the *Journal*, Haberkorn et al. (26) report their experience with PET FDG studies of patients with colorectal carcinomas receiving radiotherapy. Their group previously reported the utility of PET FDG studies in identifying recurrent colorectal carcinomas (22). In this work, they investigated the effect of radiation therapy on quantitative indices of FDG uptake in the residual primary lesions. Employing a two-ring PET system that generates three simultaneous transaxial images (two in-plane images and one cross-plane image), they studied a total of 44 patients with recurrent colorectal carcinomas after total resections of the original primary lesions. Patients were treated either with standard radiation therapy (photon source) or a combination of standard radiation therapy and neutron therapy. All patients received baseline PET FDG studies and a smaller group were evaluated up to 2 wk after photon therapy and up to 6 wk after neutron therapy.

Using a quantitative index, they refer to as the "standardized uptake value (SUV)," (defined as tissue concentration of FDG in nCi/g divided by the injected dose in nCi per body weight in g), they found that about

Received Apr. 3, 1991; accepted Apr. 3, 1991.
For reprints contact: Randall A. Hawkins, MD, PhD, Division of Nuclear Medicine and Biophysics, Department of Radiological Sciences, UCLA School of Medicine, Los Angeles, CA 90024.